Comparison of passive acoustic beamforming techniques at low-frequency using real data from an acoustic vector sensor

Eirik Rokke[1], Pietro Stinco[2], Alessandra Tesei[2], and Robert Been[2]

[1]Norwegian Defence Research Establishment (FFI), Horten, Norway
[2]NATO STO Centre for Maritime Research and Experimentation (CMRE), La Spezia, Italy

Eirik Rokke, FFI Horten, Postboks 115, 3191 Horten, Norway, eirik.rokke@ffi.no

Abstract: *The paper will compare additive and multiplicative beamforming for passive detection of low-frequency noise sources and estimation of the direction of arrival using real data collected at sea from an acoustic vector sensor mounted on a bottom node. The theory behind beamforming on acoustic vector sensors is well established in literature, for both single sensors, arrays, and spatially distributed sensors. In theory additive beamforming techniques are optimal for signal detection at low signal to noise ratio, and multiplicative processing will always be suboptimal. There are, however, advantages to multiplicative processing most notably lower processing requirements. The use of multiplicative processing is, in that sense, preferable on an autonomous system with limited processing capability, like a small bottom node. We have implemented an additive Bartlett beamformer and a multiplicative intensity based beamformer. Both methods were tested using real data from an acoustic vector sensor, the 3D GeoSpectrum M20-040, mounted on a small bottom node developed at the Centre for Maritime Research and Experimentation (CMRE). For comparison between the methods we used data from two different scenarios: A simple case with a single target moving around the bottom node within a distance of approximately 6 km and a more complex case with several targets both moving and stationary also within a distance of approximately 6 km. The paper will describe and analyse the results from both scenarios and make a quantitative comparison between the two processing methods.*

Keywords: *Acoustic vector sensor, passive acoustic.*

1. INTRODUCTION

Long-term underwater acoustic monitoring in specific areas has an important role in many civilian and defence applications, from stopping smuggling and illegal immigration to anti-submarine warfare and protection of high value assets. The use of passive acoustic surveillance in specific areas of interest may be achieved using a combination of moored and mobile underwater sensor platforms working together in a network.

In recent articles there has been several demonstrations of compact directional hydrophones, such as acoustic vector sensors (AVSs), being mounted on underwater platforms [1][2][3][4]. The AVS has the advantage of giving a frequency independent beampattern, for a wide frequency range. This is advantageous when it is mounted on a small platform, where it is not feasible to use a large array of conventional hydrophones. Centre for Maritime Research and Experimentation (CMRE) has developed a small bottom node, which is used as an experimental platform for different types of underwater sensors. A picture of the bottom node is shown in Fig. 1. For the dataset used in this paper the bottom node were equipped with two AVSs, the 3D GeoSpectrum M20-040 [5].

For this paper we used data from two different scenarios: A simple case with a single narrowband target moving around the bottom node within a distance of approximately 6 km and a more complex case with several targets both narrow- and broadband and both moving and stationary also within a distance of approximately 6 km.

There are several papers describing the theory behind different beamforming methods. For a single AVS, there are two main beamforming techniques. The first is based on additive beamforming, either conventional or adaptive [6][7][8][9]. The other method is multiplicative beamforming based on the sound intensity vector, which has information on the propagating part of the magnitude and direction of the acoustic field [10]. In theory additive beamforming techniques are optimal for signal detection at low signal to noise ratio, and multiplicative processing will always be suboptimal. There are, however, advantages to multiplicative processing most notably lower processing requirements. The use of multiplicative processing is, in that sense, preferable on an autonomous system with limited processing capability, like a small bottom node. It will therefore be of interest to see how the two different beamforming techniques preform on real data, and if it is worth using more processing power for additive beamforming.

Figure 1: Bottom node equipped with two 3D GeoSpectrum M20-040 AVSs

2. METHOD

The theory behind beamforming on acoustic vector sensors (AVS) is well established in literature, for both single sensors, arrays and spatially distributed sensors [6][8][9]. For detection of weak signals in noise, additive beamforming is the optimal approach, while for the process of localization and signal parameter estimation with higher SNR, multiplicative processing (intensity based)[9] can be advantageous. Most notably because of lower processing requirements, which is preferable on an autonomous system with limited processing capability, like a small bottom node. In this section we will first go through the required signal conditioning. Then, we will look at the theory behind the used multiplicative and additive beamforming methods. Lastly we will describe the used normalization and detection method.

2.1. SIGNAL CONDITIONING

It is necessary to do some simple conditioning of the raw-data before beamforming. The data must be conditioned for both the omni and directional channels. This is done using the known calibration values for the specific type of AVS in use [5]. Using this one gets frequency dependent calibration values for both the omni and directional channels.

The two AVSs were mounted on the bottom node with different orientations relative to eachother. To simplify the processing for the two different AVSs mounted on the bottom node, the directional channels on the AVSs are rotated into a North, East and Down (NED) coordinate system. This will make the azimuth and elevation be relative to north and up. The x, y, and z coordinate system of the AVS can easily be rotated using the yaw, pitch and roll from the non-acoustic sensors on the bottom node.

After rotating the channels into the NED coordinate system, the received signal is defined as

$$\boldsymbol{d}(t) = [v_N(t), v_E(t), v_D(t), p(t)]^T, \tag{1}$$

where p is the pressure and v is the velocity in the different directions north, east and down respectively.

2.2. MULTIPLICATIVE BEAMFORMING

Using the pressure and velocity vectors it is possible to find the direction-of-arrival (DOA) using the real part of the complex intensity vector defined as

$$\boldsymbol{I}(f,t) = 0.5\Re\{D_p(f,t)\boldsymbol{D}_v^*(f,t)\}, \tag{2}$$

where D_p is the frequency domain pressure signal and $\boldsymbol{D}_v$ is the frequency domain signal for all the velocity channels north, east and down. This vector, which is also referred to as the active intensity vector, is related to the parallel components of pressure and particle velocity and corresponds to the local net transport of sound energy. Using the inverse tangent function it is possible to measure the DOA with

$$\theta(f,t) = \text{arctan}(I_E(f,t)/I_N(f,t)), \tag{3}$$

$$\phi(f,t) = \text{arctan}\left((I_N^2(f,t) + I_E^2(f,t))^{1/2} / - I_D(f,t)\right), \tag{4}$$

where I_N, I_E and I_D are the three elements in $\boldsymbol{I}$. Bearing θ and elevation ϕ is relative to the NED coordinate system. Bearing goes clockwise with $0°$ being north and elevation goes from $0°$ being up to $180°$ being down.

2.3. ADDITIVE BEAMFORMING

Given the time domain received signal in equation 1, one can calculate the frequency domain received signal $\boldsymbol{D}(f,t)$. Using this one can define the covariance matrix as

$$\boldsymbol{R}(f,t) = \boldsymbol{D}(f,t)\boldsymbol{D}(f,t)^H, \tag{5}$$

where the superscript H is defined as conjugate transpose.

The steering vector for the AVS, dependent on the azimuth and elevation is defined as

$$\boldsymbol{w}(f,\theta,\phi) = [\cos(\theta)\sin(\phi), \sin(\theta)\sin(\phi), -\cos(\phi), 1]^T, \tag{6}$$

where azimuth, θ, is relative to north and elevation, ϕ, is relative up.

Using the defined steering vector and covariance matrix, the beampattern B can be found using a classical Bartlett beamformer

$$B(f,t,\theta,\phi) = \boldsymbol{w}^H(f,\theta,\phi)\boldsymbol{R}(f,t)\boldsymbol{w}(f,\theta,\phi). \tag{7}$$

2.4. NORMALIZATION

When using an AVS, one can in theory detect more than one target in each beampattern. This is not guaranteed and is dependent on a large angular separation between the targets. In this study we have limited ourselves to only using the maximum of the beampattern, which also makes it easier to compare the two different beamforming techniques. In Fig. 3a one can see an example off the received level for the maximum of the beampattern for time and frequency. These results include a lot of noise, and it is beneficial to normalize the spectrogram. This is done by using constant false alarm rate (CFAR) normalization by taking the mean over 1/3 seconds in time and 2 Hz in frequency. After the normalization the detections were filtered out from the noise using a threshold of 10 dB. These detections were then used to create a mask which is used on the azigram, giving the results in Fig. 3b.

3. RESULTS

As previously mentioned, we have used two different datasets for the comparison between the two methods. We will first go through the results from the simple scenario with a single target of opportunity, and then we will look at the more complex scenario with several targets.

3.1. SINGLE TARGET OF OPPORTUNITY

Fig. 2a show the scenario with a single target of opportunity. In Fig. 2b the range, azimuth and elevation for the target from the bottom node is shown. The target of opportunity is shown

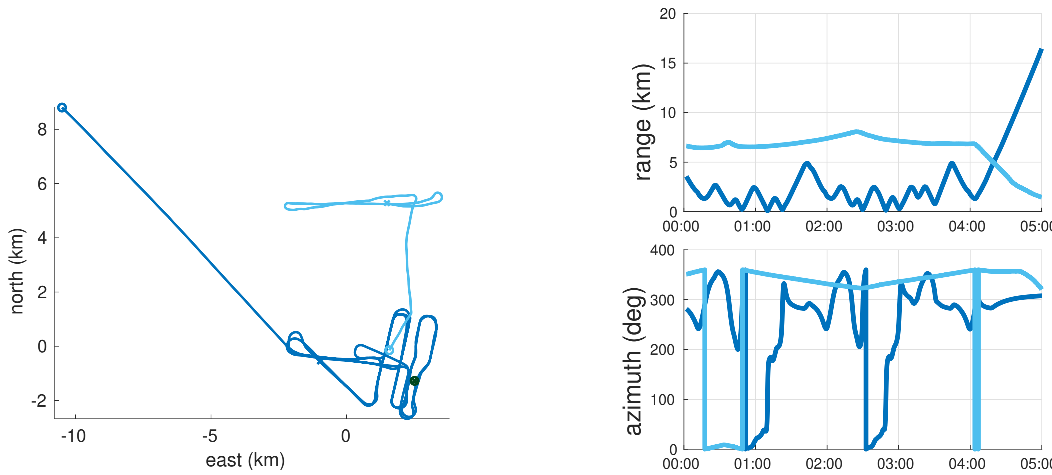

(a) Map with relevant tracks, with the bottom node in dark green.

(b) Range and azimuth from the bottom node to the two targets in the area calculated from node position and AIS.

Figure 2: Simple scenario

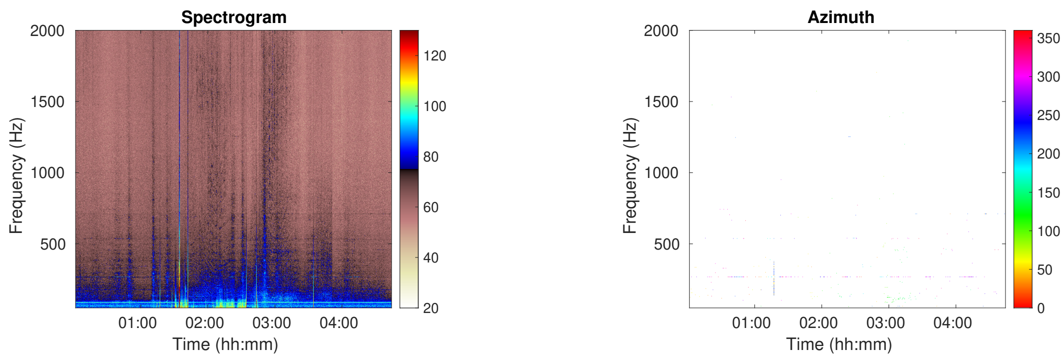

(a) Spectrogram

(b) Masked azigram using CFAR on the spectrogram

Figure 3: Beamformed results from AVS1

in dark blue, and the target in light blue was further away, very quite and the only other target in the area.

The target is known to transmit a strong frequency line and therefore the processing focuses on narrowband detection of this line. In Fig. 3a and 3b the spectrogram and CFAR-masked azigram for the processed frequency range can be seen.

These results were produced for both methods on both AVSs. Using the masked azigrams one can find the detected azimuth, for the specific frequency line, as a function of time for both methods. The ground truth from the targets AIS-data was used as a reference. Fig. 4a shows the error in measured azimuth, that is the difference between the measured azimuth of the detected target and its ground-truth. This show that the intensity and beamforming give similar results for each of the AVS.

Fig. 4b show the moving root mean square error (RMSE) of the measured azimuth. From this it is clear that the two methods on both sensors give the same uncertainty around the estimated azimuth.

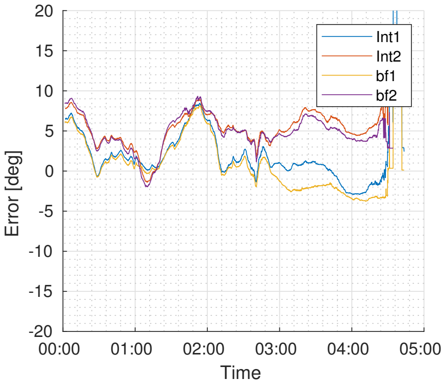

(a) *The difference between measured azimuth of the detected target and the ground truth for all the methods.*

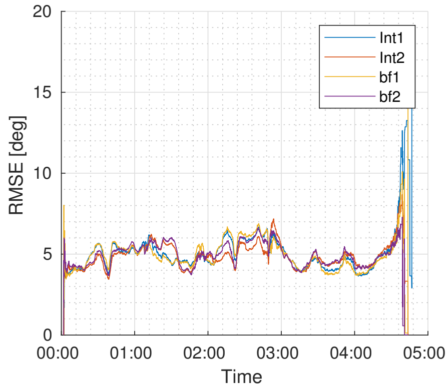

(b) *The moving RMSE of the measured azimuth for all the methods.*

Figure 4: Results for the simple scenario.

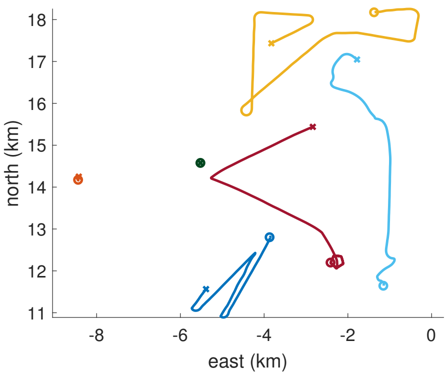

(a) *Map with relevant tracks, with the bottom node in dark green.*

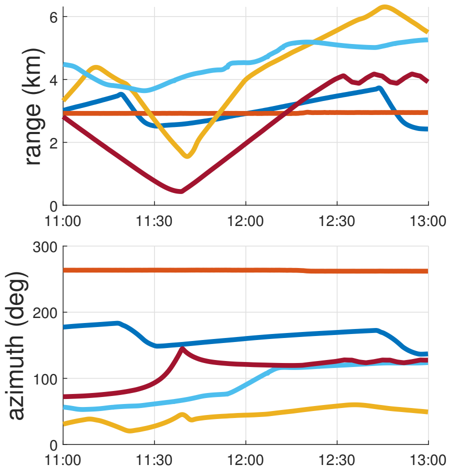

(b) *Range and azimuth from the bottom node to the two targets in the area calculated from node position and AIS.*

Figure 5: Complex scenario

3.2. COMPLEX SCENARIO WITH MANY TARGETS

In the complex scenario there were several targets, both narrow- and broadband and both moving and stationary. Fig. 5a show the scenario. In Fig. 5b the range, azimuth and elevation for the targets from the bottom node is shown.

All of these targets were detected in at least a small part of the timeframe. In this paper we will look at the results from only one of the targets, an AUV that was acting as an artificial target (dark red in Fig. 5a). The AUV was transmitting continous wave (CW) signals at 700, 1000 and 1300 Hz.

In Fig. 6a and 6b the spectrogram and CFAR-masked azigram for the processed frequency range is shown. As for the simple scenario, it is difficult to see any detections in Fig. 6b, because off the large frequency range and low amount of detections.

The same results were produced for both methods on both AVSs. Using the masked azigrams

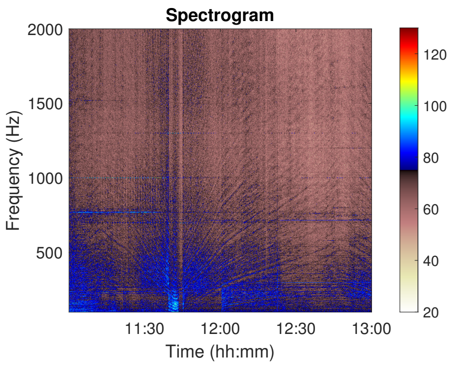

(a) Spectrogram

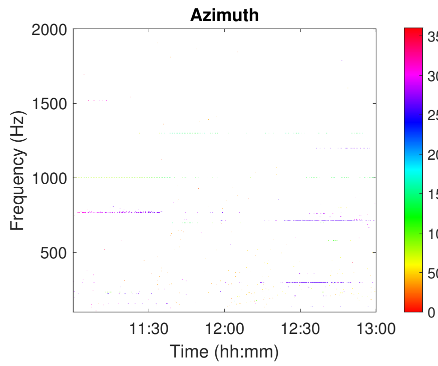

(b) Masked azigram using CFAR on the spectrogram

Figure 6: Beamformed results from first AVS

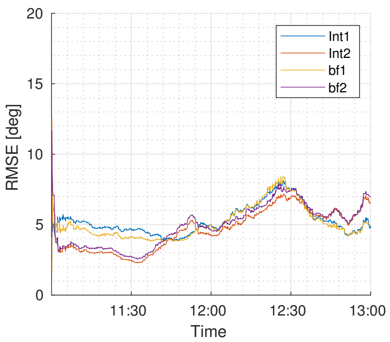

(a) 700 Hz

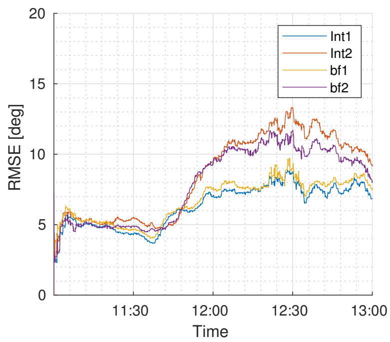

(b) 1000 Hz

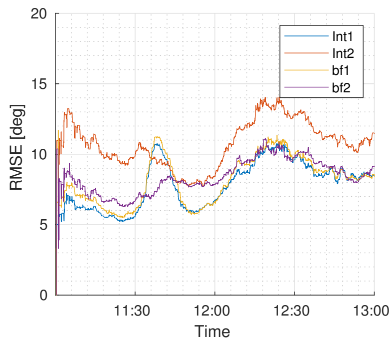

(c) 1300 Hz

Figure 7: The RMSE of the measured azimuth for the frequency lines from the target for the intensity method on AVS1 and AVS2 and the beamforming method on AVS1 and AVS2.

one can find the detected azimuth as a function of time for both methods. The ground truth from the targets AIS-data was used as a reference.

The three frequency lines transmitted by the AUV, were processed separately. Fig. 7 show the moving RMSE of the measured azimuth, for the three frequency lines. The results for the two methods on the same AVS are very similar in most of the cases. The exception is for AVS2 at 1300 Hz, where the multiplicative beamforming show significantly lower standard deviation (around 3 degrees) through most of the dataset.

4. CONCLUSION

This paper has compared additive and multiplicative beamforming for passive detection of low-frequency noise sources and estimation of the direction of arrival using real data collected at sea from acoustic vector sensors mounted on a bottom node. As described in theory the additive beamforming produces the best results, but the difference to multiplicative beamforming is not significant in most of the cases described in this paper. Except for the 1300 Hz frequency line in the complex scenario on AVS2, which seems to be an outlier. In conclusion, when comparing additive and multiplicative beamforming in both a simple and complex case. The two described methods preform almost identical when looking at the mean and standard deviation for the direction of arrival. Therefore, the use of additive beamforming is probably not worth using more off the limited processing power for real time processing on the bottom node.

REFERENCES

[1] A. Tesei, P. Stinco, R. Dreo, M. Micheli, B. Garau, R. Petroccia, D. Pinzani, A. Grati, A. Maguer : “Low-frequency passive acoustic survey of ship traffic using a glider equipped with directional sensors”, *UACE19-Greece* **(2019)**.

[2] P. Stinco, A. Tesei, G. Ferri, S. Biagini, M. Micheli, B. Garau, K.D. Lepage, L. Troiano, A. Grati, P. Guerrini : “Passive Acoustic Signal Processing at Low Frequency with a 3-D Acoustic Vector Sensor Hosted on a Buoyancy Glider”, *IEEE Journal of Oceanic Engineering* **46**, 283-293 **(2021)**.

[3] P. Stinco, A. Tesei, R. Dreo, M. Micheli : “Detection of envelope modulation and direction of arrival estimation of multiple noise sources with an acoustic vector sensor”, *Journal of the Acoustical Society of America* **149**, 1596-1608 **(2021)**.

[4] R. Dreo, A. Trabattoni, P. Stinco, M. Micheli, A. Tesei : “Detection and Localization of Multiple Ships Using Acoustic Vector Sensors on Buoyancy Gliders: Practical Design Considerations and Experimental Verifications”, *IEEE Journal of Oceanic Engineering* **48**, 577-591 **(2023)**.

[5] B. Armstrong : “Directional Hydrophones”, *Geospectrum Technical Document 2018-464* **(2018)**.

[6] A. Nehorai, E. Paldi : “Acoustic vector-sensor array processing”, *IEEE Transactions on Signal Processing* **42**, 2481-2491 **(1994)**.

[7] M. Hawkes, A. Nehorai : “Acoustic vector-sensor correlations in ambient noise”, *IEEE Journal of Oceanic Engineering* **46**, 2291 **(1998)**.

[8] M. Hawkes, A. Nehorai : “Acoustic vector-sensor beamforming and capon direction estimation”, *IEEE Transactions on Signal Processing* **26**, 337 **(2001)**.

[9] G. L. D’Spain, J. C. Luby, G. R. Wilson, R.A. Gramann : “Vector sensors and vector sensor line arrays: Comments on optimal array gain and detection”, *The Journal of the Acoustical Society of America* **120**, 171 **(2006)**.

[10] F. J. Fahy : “Sound Intensity”, (London, U.K.:E & FN Spon, 1995).